



## OPEN ACCESS

## Research paper

# Analysis of reversed halo and bullseye signs in patients with COVID-19 pneumonia on CT scan

Noor Kathem Nee'ma Al-Waely<sup>1,\*</sup>, Noor Abbas Hummadi Fayadh<sup>1</sup>, Sarah Ghaleb Shati<sup>2</sup>

## ABSTRACT

**Background:** The reversed halo sign described in the pre-COVID era in certain pulmonary pathologies, most notably cryptogenic organizing pneumonia, has been reported with varying frequency in coronavirus disease 2019 (COVID-19) pneumonia caused by the novel severe acute respiratory syndrome coronavirus 2 (SARS-CoV-2). In this study, we aimed to analyze the pattern of the reversed halo sign and its variant, the bullseye sign in patients with COVID-19 pneumonia.

**Methods:** In this study, a retrospective analysis of chest CT scans performed in the CT unit of Al-Imammain Al-Kadhymain Medical City for a three-month duration (from June to August 2020) was done. Of the 490 CT scans performed for patients with COVID-19, 330 had signs of COVID-19 pneumonia. These were evaluated for the presence of reversed halo or bullseye sign, and only obvious signs detected in at least two orthogonal planes were included. The number of these signs in each scan was documented, and an analysis of individual signs was performed. The following features were recorded; size, location, shape, and type of the peripheral rim (whether complete or incomplete, thin or thick, distinct or hazy, and uniform or non-uniform).

**Results:** A total of 26 CT exams were included in the study. The average age of the patients was  $44.85 \pm 20.14$  years, and the total number of typical reversed halo or bullseye sign lesions was 63. The rate of reversed halo/bullseye sign in this study was 7.88%. In 15 patients, the typical sign of reversed halo was seen, the bullseye sign was noted in eight patients, and three patients had both the reversed halo and bullseye signs. Nearly all the patients had other CT findings of COVID-19 pneumonia, except one with only a solitary bullseye lesion. The number of lesions ranged from one to nine with the average number of lesions per patient being 2.42. The mean size of the lesions was 3.39 cm with a size range 1–8.5 cm. Lesions were located in the periphery of the lung in most patients (93.7%). Basal predominance was seen in 76.19% patients, located in the lower lobes. A higher percent of bullseye lesions located in the upper and right middle lobes was observed ( $n = 12/23$ ) than the typical reversed halo lesions ( $n = 3/40$ ). Most lesions were oval (52.38%) or rounded (48.86%). In 77.78%, the peripheral rim was incomplete. The thickness of the peripheral rim was variable ranging from 2–19 mm. Most lesions (92.06%) exhibited a thin peripheral rim ( $<1$  cm). The rim was clearly distinct in 53.97% of lesions. It was non-uniform in thickness in most cases (95.24%).

**Conclusion:** The reversed halo sign is not infrequent among CT findings in patients with COVID-19 pneumonia. The typical reversed halo sign is more common than its variant, the bullseye sign. Variability in morphology and size does exist. In patients with COVID-19, these lesions exhibit thin, incomplete peripheral rims and are multiple in most cases.

**Keywords:** reversed halo sign, bullseye sign, COVID-19 pneumonia

<sup>1</sup>Department of Surgery-Al-Nahrain University/College of Medicine, Iraq  
<sup>2</sup>Department of Surgery-Thiqrar University/College of Medicine, Iraq  
\*Email:  
noor83kadhemi@nahrainuniv.edu.iq

<http://doi.org/10.5339/jemtac.2022.ismc.9>

Submitted: 6 April 2022

Accepted: 3 May 2022

© 2022 Al-Waely, Fayadh, Shati, licensee HBKU Press. This is an open access article distributed under the terms of the Creative Commons Attribution license CC BY-4.0, which permits unrestricted use, distribution and reproduction in any medium, provided the original work is properly cited.

## INTRODUCTION

The coronavirus disease 2019 (COVID-19) caused by the novel severe acute respiratory syndrome coronavirus<sup>2</sup> (SARS-CoV-2) spread rapidly worldwide in the past couple of years<sup>1–3</sup>. Chest computed tomography (CT) scan has a pivotal role in the primary diagnosis, evaluation of disease extent, detection of potential complications, and as a prognostic indicator in COVID-19 infection<sup>4</sup>.

Ground glass opacities (GGOs) are reported as the most frequent pulmonary parenchymal finding on a CT scan in COVID-19 pneumonia, the pattern of distribution is bilateral and peripherally predominant with basal predilection<sup>5–7</sup>.

The reversed halo sign (RHS) also known as the Atoll sign, has been described in COVID-19 pneumonia<sup>8–10</sup>. The reported frequency of this sign in patients with COVID-19 is variable, ranging from 1.7% to 15.1<sup>11</sup>.

The RHS is a patch of ground glass attenuation with a surrounding incomplete or complete ring of consolidation<sup>12</sup>. It is suggestive but not specific for cryptogenic pneumonia; moreover, it has been described in several other infectious and noninfectious pulmonary diseases<sup>13,14</sup>.

The RHS in COVID-19 is similar in morphology to that identified in organizing pneumonia. The similarity can be explained by the proposed pathogenesis of the sign. The RHS sign typically occurs long after symptom onset in the intermediate and late stages of the disease, indicating that this is a part of the underlying pathophysiology of the disease<sup>9</sup>.

A variant of RHS was described on CT scans of patients with COVID-19 and was called the bullseye sign (BES),<sup>15</sup> which is a central GGO with a surrounding air ring and an outer ring of ground-glass consolidation. The latter sign has also been described as the “target sign”<sup>16–18</sup>. The simultaneous presence of both of these signs has also been reported<sup>19</sup>.

In this study, we aimed to delineate the morphological patterns of the reversed halo and bullseye signs in patients with COVID-19 pneumonia.

## PATIENTS AND METHOD

### Study design and study population

This observational cross-sectional study included patients with COVID-19 disease referred to the CT unit at the Al-Imamain Al-Kadhymain Medical City for a period of three months from June to August 2020. All the patients had laboratory confirmation of COVID-19 infection using the reverse-transcriptase polymerase chain reaction (RT-PCR) test of nasopharyngeal swabs.

### Data collection

A total of 490 patients with COVID-19 had chest CT scans during the study period. The collection of cases was consecutive. We retrospectively analyzed the CT scans of these patients, and 330 of them had chest CT findings consistent with COVID-19 pneumonia, and these were eligible for image analysis.

### Examination protocol

The chest CT scans were performed using two multidetector scanners; a 64 scanner (SOMATOM Definition AS, Siemens Healthineers, Germany) and a 256 scanner (SOMATOM Definition Edge, Siemens Healthineers, Germany). For both scanners, the scanning parameters were a slice thickness of 1 mm with 1 mm gap and tube voltage 120 kV with automatic tube current modulation. No contrast medium was administered. The patients were examined in the supine position at the end of full inspiration when possible.

### Image interpretation

Eligible chest CT scans were analyzed for the presence of RHS or BES by two specialist radiologists. RHS was defined as an area of GGO surrounded by a complete or incomplete rim of consolidation. BES was defined as a focus of GGO surrounded by normal lung and an outer rim of consolidation or GGO. The type and number of lesions were recorded. An analysis of individual lesions was performed. The size, shape, and location of the lesions were documented. A detailed analysis of the peripheral rim included:

- Type of rim, whether complete or incomplete.
- Thickness of the rim in millimeters.
- Whether the rim was distinct or hazy. It was considered distinct if it is clearly demarcated from the internal density.
- The outline of the rim whether uniform in thickness or non-uniform (nodular).

### Statistical analysis

Microsoft Excel (Microsoft Office, 2019) was used for data analysis. Continuous data were presented as mean  $\pm$  standard deviation. Countable data were presented in frequency and percentages as tables and graphs.

## RESULTS

### Demographic data

The study included a total of 26 patients with CT scans exhibiting the typical RHS, BES, or both. The men to women ratio was 3.3:1. The mean age of the patients was  $44.85 \pm 20.14$  (28–62) years.

### Frequency of RHS and BES

The total number of lesions in all 26 patients was 63, of which 40 was RHS and 23 BES (Figure 1). The typical RHS was more frequent, observed in 15 patients, BES was seen in eight patients, and three patients had a combination of both signs (Figure 2). The overall frequency of these signs in this study was 7.88% with the frequency of typical RHS being 5.45% (18/330), and the frequency of BES being 3.33% (11/330). The number of RHS and BES for each patient ranged from 1 to 9 lesions with the average number of lesions per patient being 2.42. In the majority of patients ( $n = 25$ ), other CT findings of COVID-19 pneumonia were present. Only one patient had one BES as the only imaging manifestation of COVID-19 pneumonia (Figure 3).

### Size and shape

The average size of the lesions was 3.39 cm with a size range 1–8.3 cm. The average size of the RHS lesions was 3.49 cm, and the average size of BES was 3.22 cm. Most lesions were oval ( $n = 33$ ) or rounded ( $n = 27$ ). Only three lesions had an irregular shape (Table 1).

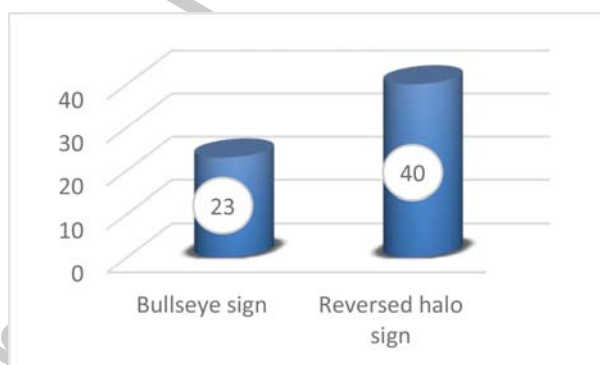


Figure 1. The number of reversed halo and bullseye signs in the study population.

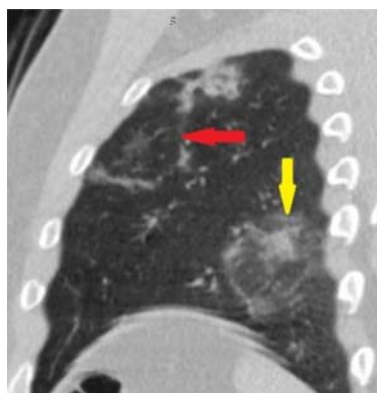
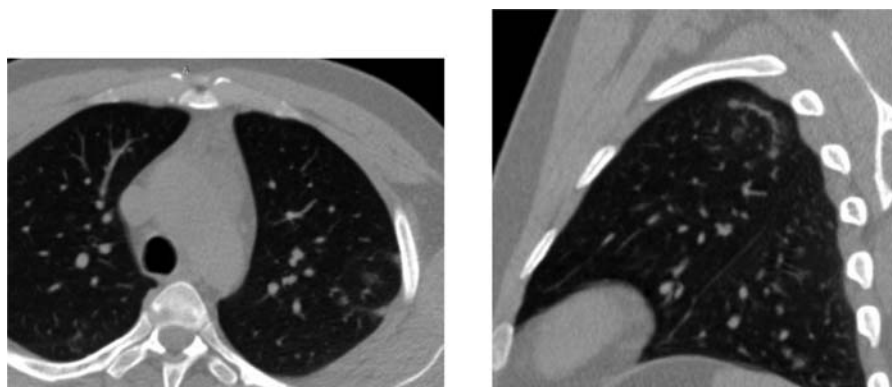


Figure 2. Sagittal reformatted chest CT scan image in a 38-year-old male patient with COVID-19 pneumonia showing the simultaneous presence of reversed halo sign (yellow arrow) and the bullseye sign (red arrow).



**Figure 3.** A-axial and B-sagittal reformatted CT scan of a 35-year-old male who presented with COVID-19 pneumonia. The images show bullseye sign in the apico-posterior segment of the left upper lobe. No additional signs of COVID-19 infection were seen in this patient.

**Table 1.** Shape of reversed halo and bullseye sign lesions.

| Shape     | Reversed halo sign (n=40) | Bullseye sign (n=23) | Total (n=63) |
|-----------|---------------------------|----------------------|--------------|
| Oval      | 26 (65)                   | 7 (30.43)            | 33 (52.38)   |
| Round     | 12 (30)                   | 15 (65.22)           | 27 (42.86)   |
| Irregular | 2 (5)                     | 1 (4.35)             | 3 (4.76)     |

Note: Data are numbers of patients with percentages in parenthesis.

#### Location of the lesions

In most cases (59/63), the lesions were located within the periphery of the lungs. Most of the lesions were pinpointed in the lower lobes (48/63). BES lesions were more frequently seen in the upper lobes and right middle lobe compared to the RHS lesions (Figure 4).

#### Analysis of the peripheral rim

The thickness of the peripheral rim was variable ranging from 2 to 19 mm with an average thickness of 5.79 mm. Most patients (92.06%) had a relatively thin peripheral rim, measuring less than 1 cm at maximum thickness. In the majority of patients, the peripheral rim was incomplete and non-uniform in thickness (Table 2).

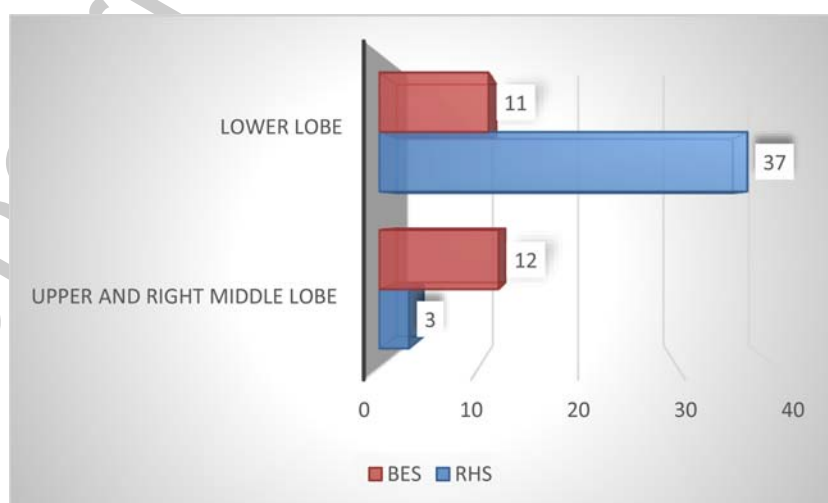


**Figure 4.** Lobar distribution of reversed halo (RHS) and bullseye (BES) signs.

**Table 2. Criteria of the peripheral rim in reversed halo and bullseye signs.**

| Criterion   | Reversed halo sign | Bullseye sign | Total      |
|-------------|--------------------|---------------|------------|
| Complete    | 11(27.5)           | 3 (13.04)     | 14 (22.22) |
| Incomplete  | 29 (72.5)          | 20 (86.94%)   | 49 (77.78) |
| Uniform     | 1 (2.5%)           | 2 (8.7)       | 3 (4.76)   |
| Non-uniform | 39 (97.5)          | 21 (91.3)     | 60 (95.24) |
| Distinct    | 17 (41.5)          | 17 (73.91)    | 34 (53.97) |
| Hazy        | 23 (57.5)          | 6 (26.09)     | 29 (46.03) |

Note: Data are numbers of patients with percentages in parenthesis.

## DISCUSSION

The RHS (Atoll sign) is frequently observed in patients with COVID-19 pneumonia. This sign has been documented in several case reports and case series published in the first few months of the global COVID-19 pandemic<sup>8,10</sup>. Later on, multiple studies addressing the CT findings in patients with COVID-19 have reported this sign with varying frequencies<sup>11</sup>. The frequency observed in this study (5.45%) was within the range reported in prior studies<sup>11</sup>. Adams et al.<sup>22</sup> reported 11.1% pooled frequency of RHS in the 28 studies included in their systematic review.

Zhang et al.<sup>23</sup> studied the postmortem histopathological changes in a patient with COVID-19 pneumonia and demonstrated changes of alveolar damage (organization phase) similar to the changes described in organizing pneumonia, and this may explain the presence of RHS in the lungs of patients with COVID-19 disease. Marchiori et al.<sup>24</sup> hypothesized another possible pathophysiologic mechanism for RHS in COVID-19 related to the presence of arterial injury, microvascular thrombi, and hypercoagulable status.

Several other signs were described as variants of RHS, including BES analyzed in this study, which has also been referred to as target sign by several authors<sup>15-17</sup>, the double halo sign<sup>25,26</sup> and the target sign described by Farias et al.<sup>27</sup> in three patients with COVID-19 which manifests as multiple concentric rings of consolidation alternating with normal lung tissue. The latter two signs (double halo and target) were not observed in our study.

In this study, multiple target-like lesions (Figure 5) were observed appearing as foci of GGO/consolidation surrounded by normal appearing lung embedded within diffuse areas of GGOs and consolidation, and these were not included in our analysis as individual lesions did not have definable walls. Another observation in our study that could not be categorized was noted in a young male patient who had multiple relatively large nodules of consolidation surrounded by very thin inner rim of normal lung and an outer rim of consolidation (Figure 6). Although this morphological pattern is similar to BES, the central area was relatively large and composed of consolidated lung rather than the GGO typically described in BES.



**Figure 5.** Axial CT scan of a young male patient showing bilateral predominantly posterior areas of consolidation involving the lower lobes and part of the lingula. Within the areas of consolidation in the lower lobes, target-like lesions (black arrows) are observed appearing as foci of consolidation surrounded by apparently normal lung tissue embedded within areas of diffuse consolidation. Note also the presence of bullseye sign (white arrow) in the subpleural location within the right middle lobe.



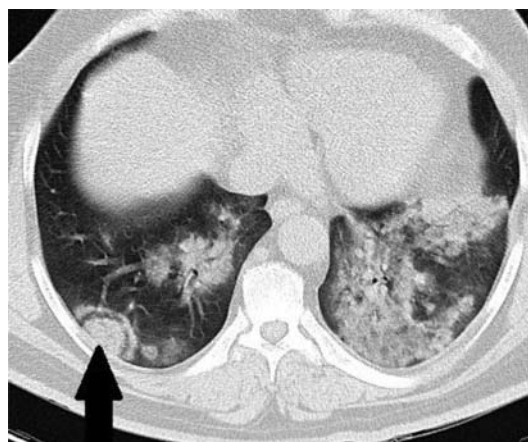


**Figure 6.** Axial CT scan of a male patient showing a lesion with target shape (black arrow) consisting of a relatively large central area of consolidation surrounded by a thin inner rim of normal lung tissue and another thin outer rim of consolidation.

Wu et al.<sup>28</sup> described the development of RHS in two patients infected with the coronavirus “delta variant”. They observed that the lesions of reversed halo showed temporal changes within days converting into areas of consolidation and ultimately either disappearing or changing into fibrous bands. In an earlier publication, Wu et al.<sup>8</sup> documented serial follow-up chest CT scans in a patient with COVID-19 pneumonia, demonstrating a pattern of organizing pneumonia with RHS developing during the time course of the patient’s illness in the late phase of the disease.

The RHS and BES observed in this study showed a great variability in size and number of lesions per patient. RHS in patients with COVID-19 show peripheral and lower lobe predominance with a thin and mostly incomplete surrounding rim of consolidation. BES, however, may be located in the central or peripheral parts of the lung with a higher percent of these lesions being observed in the upper lobes compared to RHS. The presence of either of these signs in clusters or as an isolated finding should alert the interpreting radiologist to the possibility of a COVID-19 infection. Recognizing these signs in patients with known COVID-19 disease could alter the management plan pointing to the presence of organizing pneumonia or the possibility of associated pulmonary infarction/embolism.

One limitation of this study was the lack of data regarding the timing of the CT scans in relation to the onset of the patient’s symptoms. Further studies are needed linking the presence of RHS and its variants with disease progression, prognosis, and possibly with the later development of post COVID-19 lung fibrosis.

#### REFERENCES

- [1] Zhu N, Zhang D, Wang W, et al. A novel coronavirus from patients with pneumonia in China, 2019. *N Engl J Med*. 2020;382(8):727–33. doi: [10.1056/NEJMoa2001017](https://doi.org/10.1056/NEJMoa2001017).
- [2] Tan W, Zhao X, Ma X, et al. A novel coronavirus genome identified in a cluster of pneumonia cases (Wuhan, China 2019–2020). *China CDC Wkly*. 2020;2(4):61–2.
- [3] World Health Organization. Director-General’s opening remarks at the media briefing on COVID-19 on 11 March 2020. [Internet]. WHO; 2021 [Accessed April 26, 2022]. Available from: <https://www.who.int/director-general/speeches/detail/who-director-general-s-opening-remarks-at-the-media-briefing-on-covid-19--11-march-2020>.
- [4] Kwee TC, Kwee RM. Chest CT in COVID-19: What the radiologist needs to know [published correction appears in *Radiographics*. 2022 Jan–Feb;42(1):E32]. *Radiographics*. 2020;40(7):1848–65. doi: [10.1148/rg.2020200159](https://doi.org/10.1148/rg.2020200159).
- [5] Salehi S, Abedi A, Balakrishnan S, Gholamrezanezhad A. Coronavirus disease 2019 (COVID-19): a systematic review of imaging findings in 919 patients. *AJR Am J Roentgenol*. 2020;215(1):87–93. doi: [10.2214/AJR.20.23034](https://doi.org/10.2214/AJR.20.23034).
- [6] Bayraktaroğlu S, Çinkooğlu A, Ceylan N, Savaş R. The novel coronavirus pneumonia (COVID-19): a pictorial review of chest CT features. *Diagn Interv Radiol*. 2021;27(2):188–94. doi: [10.5152/dir.2020.20304](https://doi.org/10.5152/dir.2020.20304).
- [7] Ai T, Yang Z, Hou H, et al. Correlation of chest CT and RT-PCR testing for coronavirus disease 2019 (COVID-19) in China: a report of 1014 cases. *Radiology*. 2020;296(2):E32–E40. doi: [10.1148/radiol.2020200642](https://doi.org/10.1148/radiol.2020200642).
- [8] Wu Y, Xie YL, Wang X. Longitudinal CT findings in COVID-19 pneumonia: case presenting organizing pneumonia pattern. *Radiol Cardiothorac Imaging*. 2020;2(1):e200031. doi: [10.1148/ryct.2020200031](https://doi.org/10.1148/ryct.2020200031).
- [9] Bernheim A, Mei X, Huang M, et al. Chest CT findings in coronavirus disease-19 (COVID-19): relationship to duration of infection. *Radiology*. 2020;295(3):200463. doi: [10.1148/radiol.2020200463](https://doi.org/10.1148/radiol.2020200463).
- [10] Farias LPG, Strabelli DG, Sawamura MVY. COVID-19 pneumonia and the reversed halo sign. *J Bras Pneumol*. 2020;46(2):e20200131. doi: [10.36416/1806-3756/e20200131](https://doi.org/10.36416/1806-3756/e20200131).

- 337 [11] Campagnano S, Angelini F, Fonsi GB, Novelli S, Drudi FM. Diagnostic imaging in COVID-19 pneumonia: a literature  
338 review. *J Ultrasound*. 2021;24(4):383–95. doi: [10.1007/s40477-021-00559-x](https://doi.org/10.1007/s40477-021-00559-x).
- 339 [12] Hansell DM, Bankier AA, MacMahon H, McLoud TC, Müller NL, Remy J. Fleischner Society: glossary of terms for thoracic  
340 imaging. *Radiology*. 2008;246(3):697–722. doi: [10.1148/radiol.2462070712](https://doi.org/10.1148/radiol.2462070712).
- 341 [13] Marchiori E, Zanetti G, Meirrelles GS, Escuissato DL, Souza AS Jr, Hochegger B. The reversed halo sign on high-  
342 resolution CT in infectious and noninfectious pulmonary diseases. *AJR Am J Roentgenol*. 2011;197(1):W69–W75. doi:  
343 [10.2214/AJR.10.5762](https://doi.org/10.2214/AJR.10.5762).
- 344 [14] Godoy MC, Viswanathan C, Marchiori E, et al. The reversed halo sign: update and differential diagnosis. *Br J Radiol*.  
345 2012;85(1017):1226–35. doi: [10.1259/bjir/54532316](https://doi.org/10.1259/bjir/54532316).
- 346 [15] McLaren TA, Gruden JF, Green DB. The bullseye sign: a variant of the reverse halo sign in COVID-19 pneumonia. *Clin*  
347 *Imaging*. 2020;68:191–96. doi: [10.1016/j.clinimag.2020.07.024](https://doi.org/10.1016/j.clinimag.2020.07.024).
- 348 [16] Müller CIS, Müller NL. Chest CT target sign in a couple with COVID-19 pneumonia. *Radiol Bras*. 2020;53(4):252–54. doi:  
349 [10.1590/0100-3984.2020.0089](https://doi.org/10.1590/0100-3984.2020.0089).
- 350 [17] Gomes de Farias LP, Caixeta Souza FH, da Silva Teles GB. The target sign and its variant in COVID-19 pneumonia.  
351 *Radiol Cardiothorac Imaging*. 2020;2(4):e200435. doi: [10.1148/ryct.2020200435](https://doi.org/10.1148/ryct.2020200435).
- 352 [18] Shaghghi S, Daskareh M, Irannejad M, Shaghghi M, Kamel IR. Target-shaped combined halo and reversed-halo sign,  
353 an atypical chest CT finding in COVID-19. *Clin Imaging*. 2021;69:72–4. doi: [10.1016/j.clinimag.2020.06.038](https://doi.org/10.1016/j.clinimag.2020.06.038).
- 354 [19] Giannakis A, Móré D, Mangold DL, et al. Simultaneous presence of the “bullseye” and “reversed halo” sign at CT of  
355 COVID-19 pneumonia: A case report. *Radiol Case Rep*. 2021;16(9):2442–6. doi: [10.1016/j.radcr.2021.05.074](https://doi.org/10.1016/j.radcr.2021.05.074).
- 356 [20] Li Y, Xia L. Coronavirus disease 2019 (COVID-19): role of chest CT in diagnosis and management. *AJR Am J Roentgenol*.  
357 2020;214(6):1280–6. doi: [10.2214/AJR.20.22954](https://doi.org/10.2214/AJR.20.22954).
- 358 [21] Wang J, Xu Z, Wang J, et al. CT characteristics of patients infected with 2019 novel coronavirus: association with clinical  
359 type. *Clin Radiol*. 2020;75(6):408–14. doi: [10.1016/j.crad.2020.04.001](https://doi.org/10.1016/j.crad.2020.04.001).
- 360 [22] Adams HJA, Kwee TC, Yakar D, Hope MD, Kwee RM. Chest CT imaging signature of coronavirus disease 2019 infection:  
361 in pursuit of the scientific evidence. *Chest*. 2020;158(5):1885–95. doi: [10.1016/j.chest.2020.06.025](https://doi.org/10.1016/j.chest.2020.06.025).
- 362 [23] Zhang H, Zhou P, Wei Y, et al. Histopathologic changes and SARS-CoV-2 immunostaining in the lung of a patient with  
363 COVID-19. *Ann Intern Med*. 2020;172(9):629–32. doi: [10.7326/M20-0533](https://doi.org/10.7326/M20-0533).
- 364 [24] Marchiori E, Nobre LF, Hochegger B, Zanetti G. The reversed halo sign: Considerations in the context of the COVID-19  
365 pandemic. *Thromb Res*. 2020;195:228–30. doi: [10.1016/j.thromres.2020.08.001](https://doi.org/10.1016/j.thromres.2020.08.001). Epub 2020 Aug 3. PMID: 32799128;  
366 PMCID: PMC7397932.
- 367 [25] Poerio A, Sartoni M, Lazzari G, Valli M, Morsiani M, Zompatori M. Halo, reversed halo, or both? Atypical computed  
368 tomography manifestations of coronavirus disease (COVID-19) pneumonia: The “double halo sign”. *Korean J Radiol*.  
369 2020;21(10):1161–4. doi: [10.3348/kjr.2020.0687](https://doi.org/10.3348/kjr.2020.0687).
- 370 [26] Marchiori E, Penha D, Nobre LF, Hochegger B, Zanetti G. Differences and similarities between the double halo sign,  
371 the chest CT target sign and the reversed halo sign in patients with COVID-19 pneumonia. *Korean J Radiol*.  
372 2021;22(4):672–6. doi: [10.3348/kjr.2020.1150](https://doi.org/10.3348/kjr.2020.1150).
- 373 [27] Farias LPG, Strabelli DG, Teles GBDS. COVID-19 pneumonia and target sign. *Einstein (Sao Paulo)*. 2021;19:eAl6564. doi:  
374 [10.31744/einstein\\_journal/2021Al6564](https://doi.org/10.31744/einstein_journal/2021Al6564).
- 375 [28] Wu J, Tang J, Zhang T, Chen YC, Du C. Follow-up CT of “reversed halo sign” in SARS-CoV-2 delta VOC pneumonia: A  
376 report of two cases. *J Med Virol*. 2022;94(4):1289–91. doi: [10.1002/jmv.27533](https://doi.org/10.1002/jmv.27533).
- 377  
378  
379  
380  
381  
382  
383  
384  
385  
386  
387  
388  
389  
390  
391  
392